



ozOptics

shop.ozoptics.com
www.ozoptics.com

219 Westbrook Road
Ottawa, ON, Canada, K0A 1L0

Toll-free: 1-800-361-5415
Telephone: 1-613-831-0981
Fax: 1-613-836-5089
sales@ozoptics.com

GAS-COOLED GENERATOR APPLICATIONS OF FIBER-OPTIC DISTRIBUTED STRAIN AND TEMPERATURE SENSORS

WHITE PAPER

Craig Spencer¹, Lufan Zou², George Dailey³, Omur Sezerman²

¹Calpine Corporation

²OZ Optics Limited

³QPS Photonics Inc

OZ Optics Limited, 219 Westbrook Road, Ottawa, ON, Canada, K0A 1L0
E-mail: sales@ozoptics.com | Toll free: 1-800-361-5415 | Tel: 613-831-0981 | Fax: 613-836-5089

COPYRIGHT

Copyright © 2018 by OZ Optics Ltd. All rights reserved.

OZ Optics Limited, 219 Westbrook Road, Ottawa, ON, Canada, K0A 1L0

E-mail: sales@ozoptics.com | Toll free: 1-800-361-5415 | Tel: 613-831-0981

INTRODUCTION

Modern combined cycle power plants, with state-of-art gas turbines and steam turbines coupled to air-cooled or H₂-cooled electrical generators, are highly refined technology concepts offering unmatched excellence in operation, reliability, and environmental friendliness. While generator core failures aren't common, their potential impact is up to the catastrophic level. One yet-unsolved issue is the occasional development of hot spots in the stator core, where thousands of insulated carbon steel laminates are tightly pressed and clamped together. The insulation between laminations tends to degrade in service, and foreign objects and impacts during regular maintenance outages can damage the insulation as well. Damaged insulation can cause large Eddy currents to flow leading to core damage or forced outages as the hot spots proceed to heat up and damage the bar insulation. Presently, the only methods of identifying these hot spots requires off line inspections like the ELCID, or the loop or ring flux test in conjunction with thermal imaging, but both of these tests offer challenges in correlating measured values to actual online temperatures, and neither one offers protection from emergent issues online. Current design practice does include the installation of several embedded RTDs in the core region, but these point-measuring elements are so few, and so limited in physical sensitivity range, that the probability of detecting a core issue with one is very small.

Brillouin scattering based distributed strain and temperature sensing (DSTS) provides an excellent opportunity for power generator applications, because it is unaffected by electromagnetic interference (EMI) and vibration. DSTS shows great promise in advancing core protection by permitting measurement of distributed temperatures along an entire optical fiber as the sensing element rather than at discrete points, thus achieving a true distributed sensing function. Due to the low loss of optical fibers, the sensing range can approach 100 km.

The DSTS sensor comprises a single mode optical fiber. The single mode optical fiber is contained within high strength PEEK tubing which ranges in size from 0.8 to 1.5 millimeters outer diameter. This tubing is small enough so that it can be integrated into all generator slot sizes without modifications or design changes to the generator components. The tubing can also be installed anywhere within the slot area, between top and bottom coils, on top of the top coil, or on the stator wedge surface. At certain locations a proprietary component is added to the tubing to compensate for relative thermal expansion differences between the optical fiber and generator components, which enables measurement of true temperature or strain. The PEEK tubing can be placed in direct contact with the stator laminations, stator coil groundwall, or both simultaneously.

This paper presents a brief description of the DSTS principle of operation, and discusses the results of generator stator temperature monitoring tests that used an OZ Optics Ltd. DSTS product, and were performed in a Siemens air-cooled generator and a GE H₂-cooled generator owned by Calpine Corporation.

PRINCIPLE OF OPERATION

BRILLOUIN OPTICAL TIME-DOMAIN ANALYSIS (BOTDA)

Brillouin scattering stems from the density variations that dielectric materials exhibit in the presence of an electric field¹. If an optical signal, called a probe, is injected into one end of an optical fiber, and a strong optical signal, called a pump, is injected into the other end, then the density variations induced by the electric field of the pump will result in a distributed refractive index grating inside the fiber. The distributed grating will, in turn, cause the probe to scatter in the backward direction, as shown in Figure 1.

¹ This phenomenon is called electrostriction.

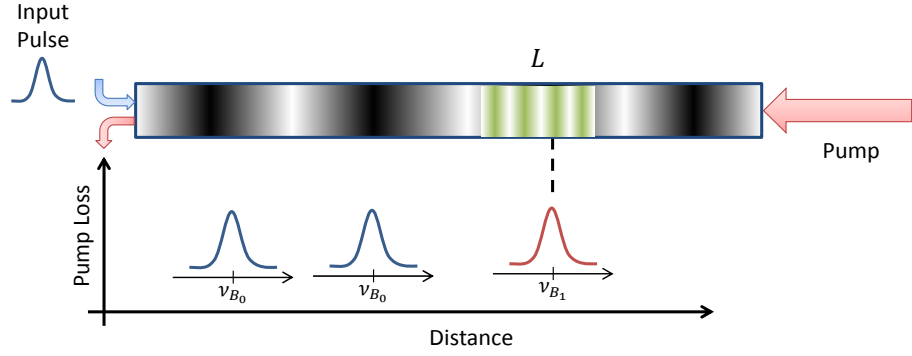


Figure 1. Brillouin scattering sensing principle.

The scattered signal is shifted in frequency by an amount ν_{B0} called the Brillouin frequency shift. For standard single-mode fibers, operated at a wavelength of $1.55 \mu\text{m}$, the Brillouin frequency shift is approximately 11GHz. If a section of the optical fiber is stressed either mechanically or thermally, the Brillouin frequency shift of the scattered light from that fiber section, noted as ν_B , will be different from the Brillouin frequency shift of the unstressed fiber. The amount of change in the Brillouin frequency shift is proportional to the change in temperature and/or strain. This linear dependency is typically written as [1, 2]:

$$\nu_B(T_0, \varepsilon) = C_\varepsilon (\varepsilon - \varepsilon_0) + \nu_{B0}(T_0, \varepsilon_0) \quad (1)$$

$$\nu_B(T, \varepsilon_0) = C_T (T - T_0) + \nu_{B0}(T_0, \varepsilon_0) \quad (2)$$

where C_ε and C_T are the optical fiber strain and temperature coefficients, respectively, and ε_0 and T_0 are the strain and temperature corresponding to a reference Brillouin frequency ν_{B0} . For instance, laboratory measurements on ITU G.652 (SMF-28) fibers yielded the values of $C_\varepsilon = 0.0529 \text{ MHz}/\mu\text{e}$ and $C_T = 1.0241 \text{ MHz}/^\circ\text{C}$.

The BOTDA system, whose block diagram is shown in Figure 2, is based on the interaction through Brillouin scattering of a pulsed laser, acting as a probe, with a counter-propagating continuous-wave (CW) pump laser. The probe beam exhibits Brillouin amplification at the expense of the CW beam. The resultant power drop in the CW beam is measured while the frequency difference between two lasers is scanned, giving the Brillouin loss spectrum of the sensing fiber. The shift in the Brillouin spectrum of the fiber is used to calculate the temperature and/or strain change of the sensing fiber.

The BOTDA system has many features allowing it to achieve spatial resolutions as small as 10 cm [3], and to cover sensing lengths as large as 100 km. In addition, it can achieve high temperature and strain measurement accuracies of $\pm 0.1 \text{ }^\circ\text{C}$ and $\pm 2 \mu\text{e}$, respectively.

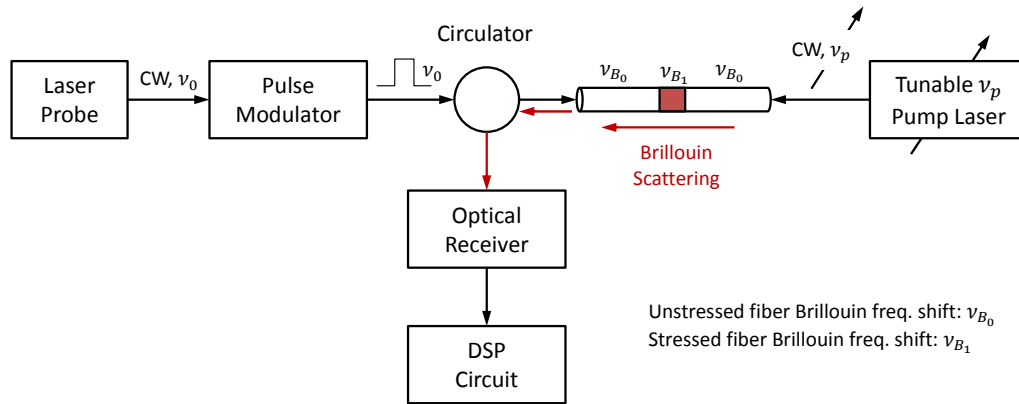


Figure 2. BOTDA block diagram.

EXPERIMENT GOAL

The overall goal of the experimental procedure was to assess the temperature monitoring capabilities of the BOTDA technology with the sensing medium of optical fibers located on the stators. To achieve this goal, field tests were conducted in a Siemens air-cooled generator in Hermiston, OR, USA and a GE H₂-cooled generator in Hidalgo, TX, USA operated by Calpine Corporation in October 2017 and June 2018, respectively.

EXPERIMENTAL SETUP

1) SIEMENS OPEN AIR COOLED GENERATOR

A proof-of-concept application was installed firstly into Calpine's Hermiston CTG1 Siemens Westinghouse – AeroPac I – Open Air Cooled generator as shown in Figure 3. Figure 4 displays the sensing fiber installed on top of the stator wedges.

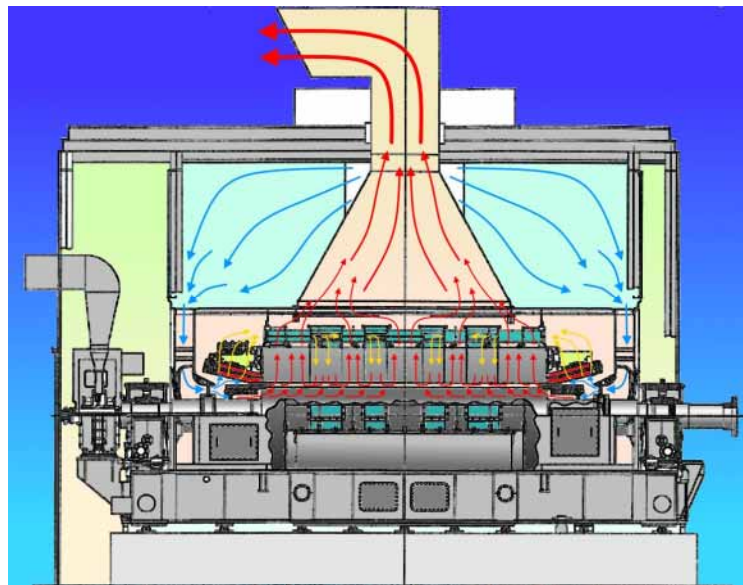


Figure 3. Siemens Westinghouse – AeroPac I – Open Air Cooled generator.

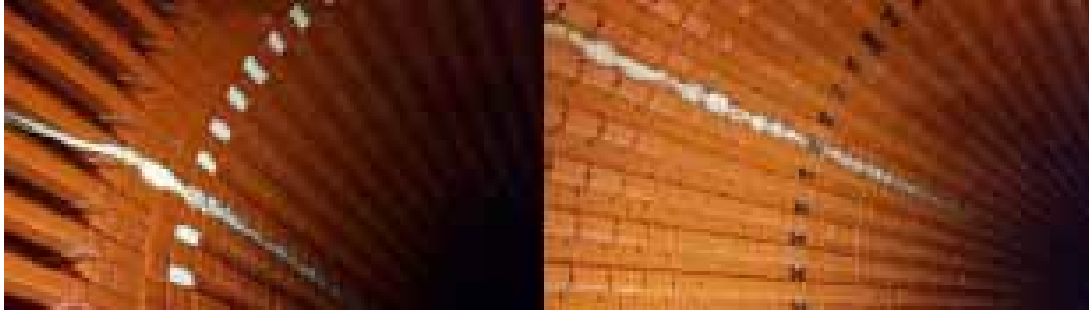


Figure 4. Sensing fiber installed on top of the stator wedges.

2) GE H₂-COOLED GENERATOR

The 2nd BOTDA application for a power generator was installed into Calpine's Hidalgo CTG1 GE H₂-Cooled generator as shown in Figure 5. Figure 6 displays the sensing fiber installed under the wedges in the base shim stock.

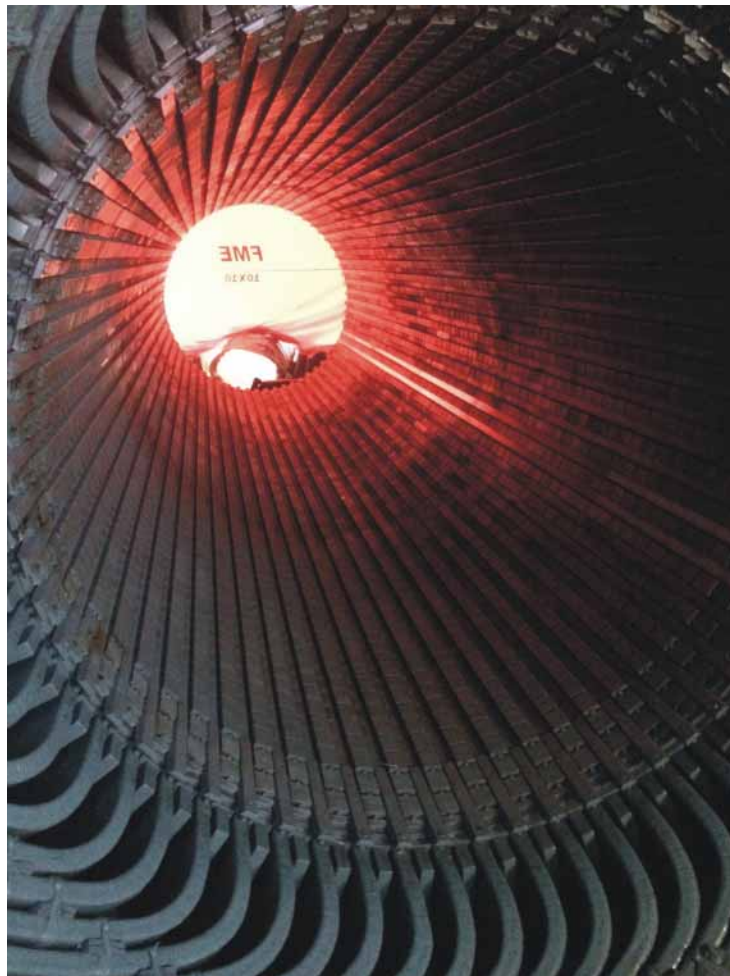


Figure 5. GE H₂-Cooled generator.

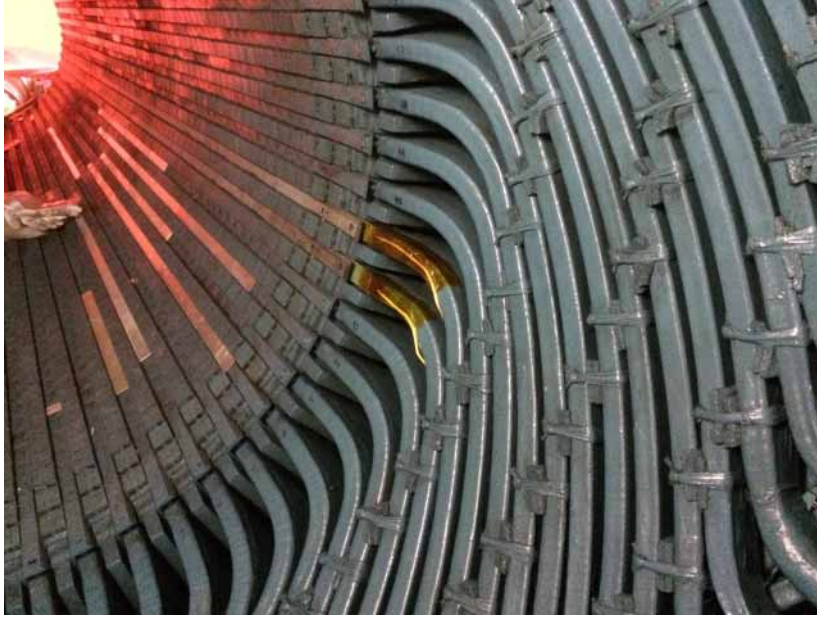


Figure 6. Sensing fiber installed under the wedges in the base shim stock.

RESULTS

In these tests, the temperature change with power loading change (relative to the Brillouin frequency shift, ν_{B0} , on the reference without power loading) was recorded and analyzed.

1) SIEMENS OPEN AIR COOLED GENERATOR

Figure 7 displays temperature distributions along the sensing fiber installed on top of the stator wedges when the power loading increased from 25MVA to 170MVA. The sensing fiber went through the stator slot twice to become a loop-back configuration, with the loop-back point shown at the cursor location in the data and pointed out in the inserted photo. Using the cursor as a mirror and moving right and left curves together, the temperature distributions emerge which clearly demonstrated the stator zone-cooling temperature affects along the length of the fiber as shown in Figure 8.

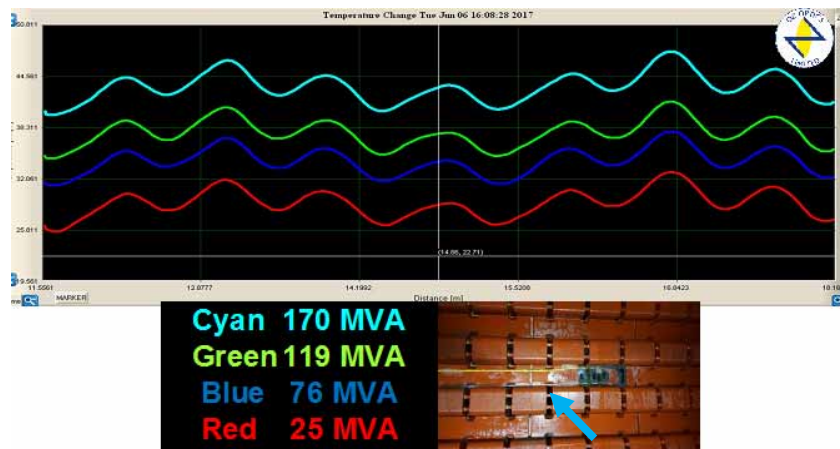


Figure 7. Temperature distributions when the power loading increased from 25MVA to 170MVA.

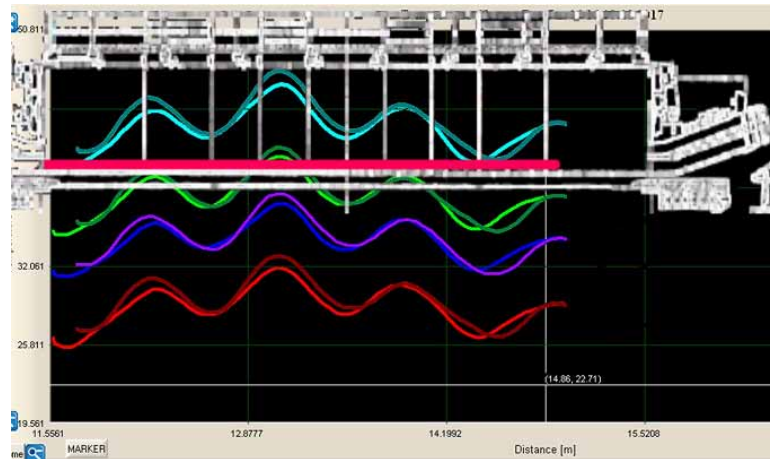


Figure 8. Temperature distributions measured by BOTDA that clearly demonstrated the stator zone-cooling temperature affects along the length of the fiber.

Once online, temperature readings (related to 21.5°C baseline) from the fiber optic line (DSTS) compared well against the existing RTD readings. The DSTS readings are hotter than the measured hot air (exhaust) temperature, indicating localized sensing of the temperature. The DSTS readings are cooler than the embedded RTD readings. This is expected because the embedded RTDs are radially deeper in the slots and are therefore less exposed to cooling air flow than where the DSTS sensor was. The wavy patterns in the temperature data along the length of the fiber correlate well to the different zone-cooled regions of the core, where the ventilation flow is moving radially inward or radially outward depending on the zone in the core, and the temperature of each particular zone varies based on its flow path and the amount of heat the air flow has absorbed.

The one exception to the trends noted above is at the 26 MVA rating, where the DSTS registered a higher temperature than the embedded RTDs. This is likely due to the relatively quick ramping up through the 26 MVA point. Early in operation, heat hasn't yet saturated the thermal mass of the core

Comparison with RTDs and OZ DSTS Data						
Load	Cold Air	Hot Air	Embedd ed	Av. Trough*	Av. Peak*	OZ DSTS
170 MVA	30.6°C	64.4°C	78.1°C	63.9°C	67.0°C	68.0 °C
119 MVA	28.6°C	57.8°C	64.1°C	58.3°C	61.3°C	62.2 °C
26 MVA	21.6°C	45.6°C	45.3°C	49.9°C	52.7°C	53.5 °C

2) GE H₂-COOLED GENERATOR

While waiting on site for a generator to be brought online to test the next generator installation of the DSTS sensor, OZ Optics performed a bench test of the DSTS system to demonstrate its ability to detect highly localized heat sources. P.J. Tavner and A.F. Anderson [4] in their article on core failures state that “core faults usually, but not always, occur in the stator” and “core faults tend not to grow unless the initiating defect is >1 cm in diameter.” Since

the spatial resolution of all current fiber optic distributed temperature sensors is not better than 10 cm, a 1 cm aluminum block, as shown in Figure 9, was used to verify that the OZ DSTS has the capability to detect a 1 cm long hotspot. A certain length of fiber was coiled up before insertion into the block, and the remainder of 1 km fiber was spliced into the inserted fiber on the other side of the block. The fiber ran through a 1/16" PEEK plastic tube embedded in the block, so it was not in direct contact with the aluminum to approximate an actual generator installation configuration. Figure 10 displays the temperature measurements relative to a room temperature of 22.3°C when the temperature increased from 52.2°C to 100°C. The hotspot located around 204.40m can be easily found when the temperature change is over 30°C (52.2°C - 22.3°C) within a 1 km length as shown in Figure 11.

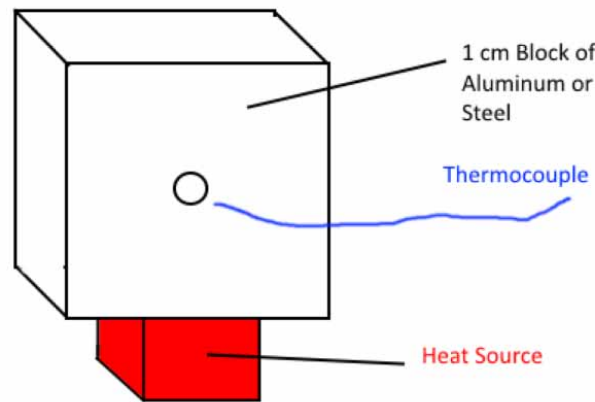


Figure 9. Schematic of 1cm hotspot.

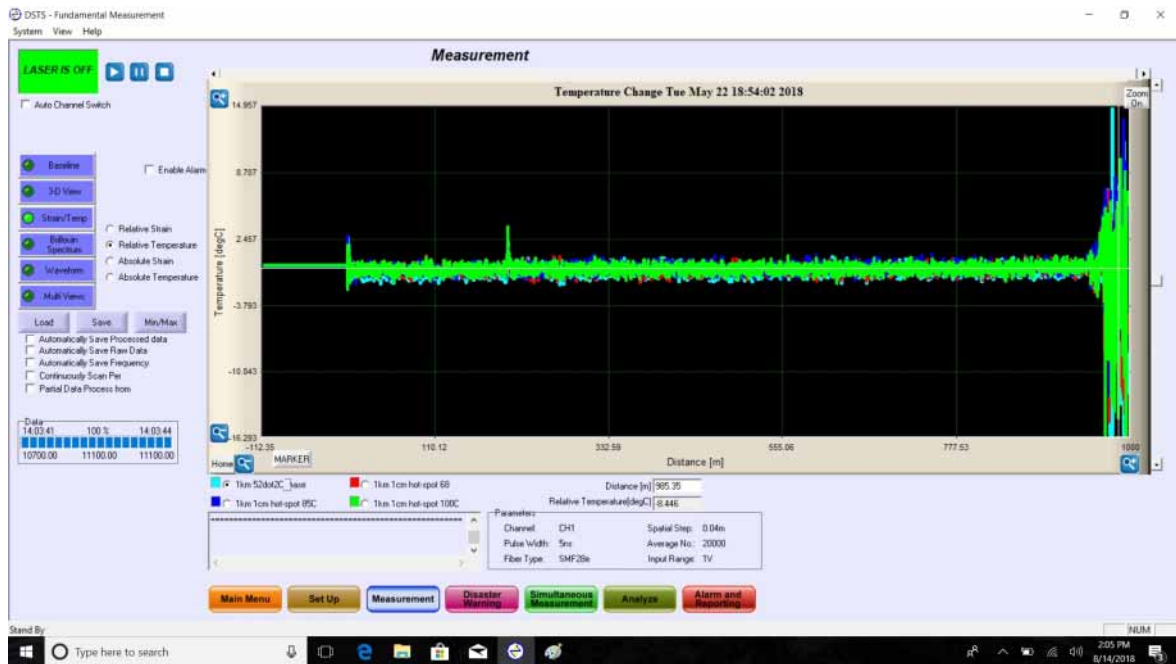


Figure 10. Within a 1 km fiber a 1 cm hotspot was measured relative to a room temperature of 22.3°C, when the temperature increased from 52.2°C to 100°C.

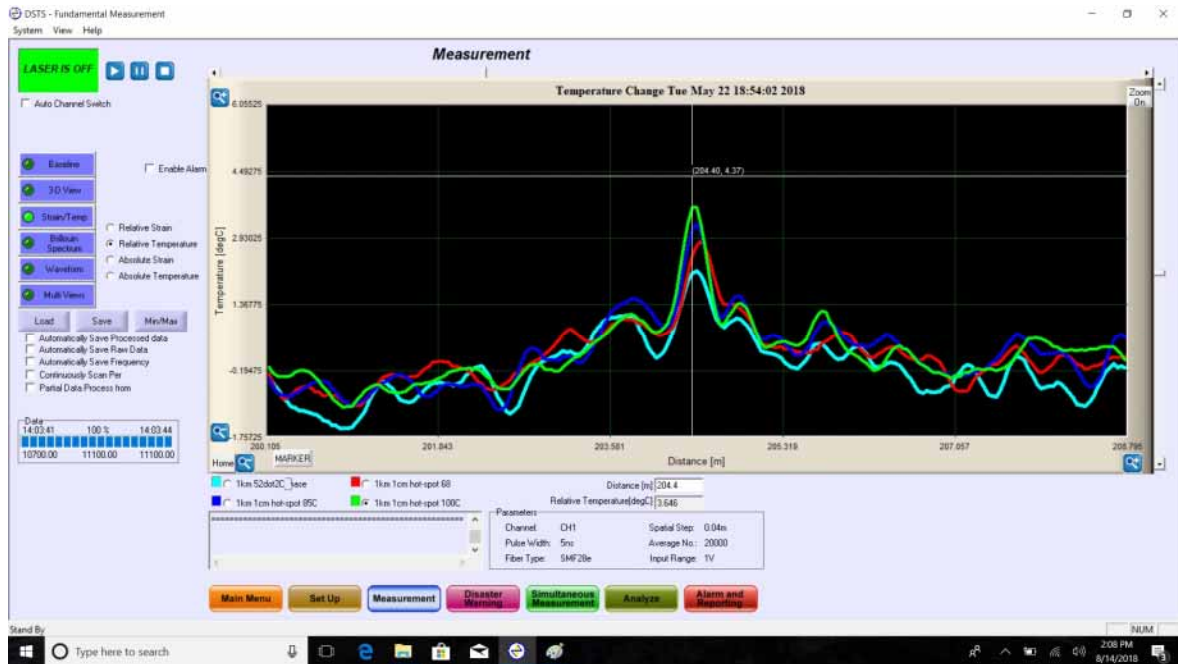


Figure 11. Hotspot located around 204.40 m can be easily found when the temperature change is over 30°C (light blue, red, blue, and green for 52.2, 68.0, 85.0, and 100°C, respectively) within 1 km distance.

Now returning focus to generator testing, note that the cooling system of this generator is different from the air-cooled generator above. This generator utilizes pressurized H₂ contained within the generator frame as its cooling medium, and the physical dimensions of the unit and the layout of its ventilation flow are somewhat different designs. Despite size and layout differences, this generator utilizes a zone-cooled core and has a blower on each end just like the generator above, so we would expect to find a somewhat similar curve to the generator above, with corresponding wavy temperature deviations along the length of the sensor and a relatively cooler slot entrance/exit region.

Figure 12 displays the temperature distributions along the sensing fiber, which was installed under the wedges in the base shim stock, falling well in line with expectations. The cursor denotes the loop-back point located at 273.91 meters. Curves are plotted for four different load points, ranging from 94.6 MVA to 154.0 MVA .



Figure 12. Temperature distributions matched well against the existing RTD readings.

You will notice in the plots, above, the wavy temperature distribution is approximately symmetric about the loop-back point, coupled with the relatively cooler locations at the ends and near the loop-back, which correspond to slot entrances/exits.

Unlike the first generator where the fibers were almost directly influenced by ventilation flow due to the installation location, the fibers in this generator were largely removed from direct ventilation with the exception of the radial vents at the core. Additionally, the heating profile of the stator core is most intense in close proximity to the inner-diameter tips of the stator slots. These factors combine to predict that the measured temperatures would be higher than the embedded RTDs, which are both further away radially from the tips of the stator slots and circumferentially positioned away from the core iron on the order of 1 cm or more. This is what we have observed in the test data which is tabulated below, with temperature readings in centigrade.

MW	MVAR	MVA	Cold Gas	Hot Gas	Embedded RTD	OZ DSTS
132.4	8.3	132.7	36.0	46.1	54.8	55.8
152.2	23.2	154.0	38.2	48.9	58.5	60.2
151.0	27.4	153.5	38.2	49.4	59.1	61.2
111.2	26.4	114.3	38.2	48.9	56.5	58.5
90.2	28.4	94.6	36.7	45.6	48.9	51.8

CONCLUSION

DSTS technology has proven to be an efficient and cost-effective solution to monitor temperatures in electrical generators. Furthermore, while the resolution is defined as 10 cm, DSTS technology can detect hot spots only 1 cm in length when the temperature changes over 30°C, opening the possibility for software solutions to define alarm and trip points to mitigate localized core damage which may occur during operation. The online temperature readings from the fiber optic line compared well against the existing RTD readings. More importantly, beautiful data curves emerged which clearly demonstrated the stator zone-cooling temperature affects along the length of the fiber installed in these generators.

Overall, the results were very encouraging for developing advanced online core thermal protection, as well as for additional applications of distributed temperature sensing for electrical generators with a useful long-term, proactive monitoring platform.

REFERENCES

- [1] Horiguchi, T., Kurashima, T. and Tateda, M., "Tensile strain dependence of Brillouin frequency shift in silica optical fibers," *IEEE Photon. Tech. Lett.* 1, 107-108 (1989).
- [2] Kurashima, T., Horiguchi, T. and Tateda, M., "Thermal effects on Brillouin frequency shift in jacketed optical silica fibers," *Appl. Opt.* 29, 2219-2222 (1990).
- [3] Zou, L., Bao, X., Wan, Y. and Chen, L., Coherent probe-pump based Brillouin sensor for centimeter-crack detection, *Opt. Lett.* 30, 370-372 (2005).
- [4] Tavner, P.J. and Anderson A.F., "Core faults in large generators," *IEE Proc.-Electr. Power Appl.*, Vol. 152, No. 6, 1417-1439 (2005).